0026-895X/06/7003-818–828$20.00
MOLECULAR PHARMACOLOGY
Copyright © 2006 The American Society for Pharmacology and Experimental Therapeutics
Mol Pharmacol 70:818–828, 2006

Vol. 70, No. 3
21717/3132811
Printed in U.S.A.

Target Soluble *N*-Ethylmaleimide-Sensitive Factor Attachment Protein Receptors (*t*-SNAREs) Differently Regulate Activation and Inactivation Gating of Kv2.2 and Kv2.1: Implications on Pancreatic Islet Cell Kv Channels

Tami Wolf-Goldberg, Izhak Michaelevski, Laura Sheu, Herbert Y. Gaisano, Dodo Chikvashvili, and Ilana Lotan

Department of Physiology and Pharmacology, Sackler Faculty of Medicine, Tel-Aviv University, Ramat-Aviv (T.W-G., I.M., D.C., I.L.); and Departments of Physiology and Medicine, University of Toronto, Toronto, Ontario, Canada (L.S., H.Y.G.)

Received December 18, 2005; accepted May 31, 2006

ABSTRACT

We have hypothesized that the plasma membrane protein components of the exocytotic soluble *N*-ethylmaleimide-sensitive factor attachment protein (SNAP) receptor (SNARE) complex, syntaxin 1A and SNAP-25, distinctly regulate different voltage-gated K^+ (Kv) channels that are differentially distributed. Neuroendocrine islet cells (α, β, δ) uniformly contain both syntaxin 1A and SNAP-25. However, using immunohistochemistry, we show that the different pancreatic islet cells contain distinct dominant Kv channels, including Kv2.1 in β cells and Kv2.2 in α and δ cells, whose interactions with the SNARE proteins would, respectively regulate insulin, glucagon and somatostatin secretion. We therefore examined the regulation by syntaxin 1A and SNAP-25 of these two channels. We have shown that Kv2.1 interacts with syntaxin 1A and SNAP-25 and, based on studies in oocytes, suggested a model of two distinct modes of interaction of syntaxin 1A and the complex syntaxin 1A/SNAP-25 with the C terminus of the channel. Here, we characterized the interactions of syntaxin 1A and SNAP-25 with Kv2.2 which is highly homologous to Kv2.1, except for the C-terminus. Comparative two-electrode voltage clamp analysis in oocytes between Kv2.2 and Kv2.1 shows that Kv2.2 interacts only with syntaxin 1A and, in contrast to Kv2.1, it does not interact with the syntaxin 1A/SNAP-25 complex and hence is not sensitive to the assembly/disassembly state of the complex. The distinct regulation of these closely related channels by SNAREs may be attributed to differences in their C termini. Together with the differential distribution of these channels among islet cells, their distinct regulation suggests that the documented profound down-regulation of islet SNARE levels in diabetes could distort islet cell ion channels and secretory responses in different ways, ultimately contributing to the abnormal glucose homeostasis.

Secretion in neurons and neuroendocrine cells are regulated by SNARE proteins. These SNARE proteins, particularly the two plasma membrane associated (t-SNAREs), syntaxin 1A and SNAP-25, regulate not only exocytosis per se but also directly modulate calcium (for reviews, see Catterall, 2000; Spafford et al., 2003) and potassium channels, including Kv (Fili et al., 2001; Ji et al., 2002; Leung et al., 2003; Michaelevski et al., 2003) and K_{ATP} channels (Kang et al., 2004; Pasyk et al., 2004). Whereas these SNARE proteins bind highly conserved domains (II-III cytoplasmic loop) within the family of calcium channels (for review, see Spafford et al., 2003), we have noted that the SNARE proteins bind the different Kv channel members, particularly Kv1.1 and Kv2.1, at distinct domains of their cytoplasmic N and C termini (Fili et al., 2001; Michaelevski et al., 2002). These reports raise the hypothesis that these SNARE proteins are capable of distinct regulation of different Kv channel members that are differentially distributed within a single cell type (neuron) or within adjacent interacting cell types, which would thereby more versatilely influence their electrical plasticity and intercellular communication. The most notable examples of the latter are the brain and the pancreatic islet.

This work was supported by grants from the United States-Israel Binational Science Foundation (to I.L.), the Israel Academy of Sciences (to I.L.), the State of Israel Ministry of Health (to I.L.) the US-Israel Binational Foundation (to I.L.), Canadian Institute of Health Research MOP-69083 (to H.G.), and Juvenile Diabetes Research Foundation 1-2005-1112 (to H.G.).

T.W.-G., I.M., and L.S. contributed equally to this work.

Article, publication date, and citation information can be found at http://molpharm.aspetjournals.org.

doi:10.1124/mol.105.021717.

ABBREVIATIONS: SNARE, SNAP receptor; t-SNARE, target SNARE; SNAP, soluble *N*-ethylmaleimide-sensitive factor attachment protein; HEK, human embryonic kidney; BoNT/A, Botulinum neurotoxin A; AS-ODN, antisense oligodeoxynucleotide; Ab, antibody; IP, immunoprecipitated; IB, immunoblotted; PAGE, polyacrylamide gel electrophoresis; RCF, residual current fraction; NS, nonsense.

The pancreatic islet consists of several cell types, including α, β, and δ cells, that assert intimate paracrine regulation over each other via their major secretory products to very finely regulate glucose homeostasis (Cejvan et al., 2003; Ishihara et al., 2003; Wendt et al., 2004). It is noteworthy that it has been suggested (based mainly on analysis at the mRNA level) that in the human pancreatic islet, the different islet cells contain distinct dominant Kv channels, including Kv3.1 in α cells, Kv2.1 in β cells, and Kv2.2 in δ cells, which would regulate secretion of glucagon, insulin, and somatostatin, respectively (Yan et al., 2004). All these islet cells contain syntaxin 1A and SNAP-25 (Wheeler et al., 1996); remarkably, in human and rodent type-2 diabetes, islet expression of these SNARE proteins are profoundly down-regulated, which we believe would distort the different islet cell ion channels and secretory responses, ultimately contributing to the abnormal glucose homeostasis (Chan et al., 1999; Gaisano et al., 2002; Ostenson et al., 2006). Here, we tested this hypothesis by examining the SNARE complex regulation of the closely related Kv2.1 and Kv2.2 channels. First, we demonstrated the localization of the Kv2.2 protein to human and rat δ and not β cells and, vice versa, the localization of the Kv2.1 protein to β and not δ cells. Islet β cells are abundant, constituting ~70% of the islet cells, so that we could previously demonstrate the interaction of Kv2.1 channel with syntaxin 1A and SNAP-25 in these cells (MacDonald et al., 2002; Leung et al., 2003). However, δ cells are quite sparse, constituting <5% of islet cells, and are thus very difficult to examine (Kanno et al., 2002). We have therefore used the heterologous *Xenopus laevis* oocyte model to analyze the precise syntaxin 1A and SNAP-25 interactions with islet Kv channels Kv2.1 and Kv2.2.

We have previously characterized the interactions of syntaxin 1A and SNAP-25 with Kv2.1 (Michaelevski et al., 2003). We showed that both activation and inactivation of the channel were affected, depending on the assembly/disassembly of the syntaxin/SNAP-25 complex. On the basis of these results, we suggested a model that describes the modes of interaction of Kv2.1 with syntaxin 1A and with syntaxin 1A/SNAP-25. Furthermore, two sets of data indicated that the C terminus of Kv2.1 may play an important role in these interactions. First, in vitro binding assays have shown that syntaxin 1A and the syntaxin/SNAP-25 complex bind directly to the C terminus of the channel (Michaelevski et al., 2003; Tsuk et al., 2005). Second, the functional interactions were abolished by both C-terminal deletions and by the presence of dominant-negative C-terminal peptides (Tsuk et al., 2005). In this study, we characterized the functional and physical interactions of syntaxin 1A and SNAP-25 with Kv2.2, which is highly homologous to Kv2.1, except for its C terminus, which is the *t*-SNAREs interacting region. Comparison between Kv2.2 and Kv2.1 highlights different interactions of the *t*-SNAREs with these two channels. This study demonstrates that though these *t*-SNARE proteins are well conserved between interacting islet cells (and presumably adjacent distinct brain neurons), they nonetheless exert profoundly distinct actions on even closely related Kv channel isoforms.

Materials and Methods

Constructs and Antibodies. The primary antibodies used were: polyclonal syntaxin 1A (Alomone Labs, Jerusalem, Israel); monoclonal SNAP-25 (BD Transduction Laboratories, Lexington, KY), polyclonal Kv2.1 and polyclonal Kv2.2 (Alamone Labs; see below for their characterization). Kv2.1 cDNA was either cloned in pBluescript (kindly donated by Prof. R. Joho, The University of Texas Southwestern Medical Center, Dallas, TX) for oocyte injection, or in pcDNA3, for HEK-293 cells transfection. Kv2.2 (kindly donated by Prof. O. Pongs, University of Hamburg, Hamburg, Germany), syntaxin 1A and SNAP-25 (kindly donated by E. Isacoff, University of California, Berkeley, CA) cDNAs were subcloned in pGEMHE for oocyte injection or in pcDNA3 for HEK-293 transfection. Botulinum neurotoxin A (BoNT/A) light-chain cDNA (Huang et al., 2001) were subcloned in pCDNA3. Preparation of mRNAs was as described previously (Levin et al., 1996). Materials and enzymes for molecular biology were purchased from Roche Diagnostics (Mannheim, Germany), Promega (Madison, WI), and MBI Fermentas (Vilnius, Lithuania). The degenerate phosphorothioate antisense oligodeoxynucleotides (AS-ODNs) (including 5′ and 3′ end capping of 2- and 4-phosphorothioates, respectively, and a phosphorothioate at every third internal position to enhance nuclease resistance) were targeted against the following degenerate (Xy denotes three parts of X and one part of y) nucleotide sequences corresponding to SNAP-25: ANSP-1, 5′GATGA(Ga)TC-(Ca)(Ct)T(Gc)GA(GA)AG(CT)AC(Cg)CGNCGNATGCT3′ (encoding amino acids DESLESTRRML); and ANSP-2, 5′A(CT)GA(Ag)(GA)-A(TC)GA(AG)ATGGANGA(AG)AA(Ct)(Cta)T 3′ (encoding amino acids REDEMEEN).

Characterization of Kv2.1- and Kv2.2-Specific Antibodies. We characterized a new affinity-purified antibody (N-terminal Ab) directed against an N-terminal peptide sequence of Kv2.1 (amino acids 4–26) that is highly homologous to a corresponding peptide in Kv2.2 (Alomone Labs, not available commercially), and compared it with the antibody directed against a unique C-terminal peptide sequence of Kv2.1 (C-terminal Ab; Alomone Labs). The C-terminal Ab, as expected (Michaelevski et al., 2003), recognized only Kv2.1 and not Kv2.2. In contrast, the N-terminal Ab, peculiarly, recognized only Kv2.2, not Kv2.1. Thus, in rat brain lysate (Fig. 1A, left) the N-terminal Ab did not recognize Kv2.1 that was recognized by the C-terminal Ab. However, it recognized higher molecular mass doublet of proteins [the calculated molecular mass of Kv2.2 (102.11 kDa) is higher than that of Kv2.1 (95.2 kDa)]; the lower band migrated as a Kv2.2 protein expressed in oocytes (Fig. 1B, left); the upper band may correspond to a post translationally processed (e.g., highly glycosylated) form of the protein. In addition, in PC-12 cells (Fig. 1A, right), the N-terminal Ab neither immunoprecipitated (IP) Kv2.1, which was precipitated by the C-terminal Ab nor immunoblotted (IB) Kv2.1 that was precipitated by the C-terminal Ab (at very long exposures, however, a very faint band corresponding to Kv2.1 could be resolved). However, the N-terminal Ab could both precipitate and blot what seems to be Kv2.2, as expected. In accord, in the heterologous expression system of *Xenopus laevis* oocytes, the N-terminal Ab blotted only expressed Kv2.2 but not Kv2.1 (Fig. 1B, right). However, it precipitated both Kv2.1 and Kv2.2 (Fig. 1B, left), in contrast to the results in PC-12 cells. A plausible explanation for the discrepancy may be that the large concentration of overexpressed channels in oocytes "overcomes" the low affinity of the N-terminal Ab to Kv2.1. We concluded that the N- and C-terminal Abs can differentially recognize Kv2.2 and Kv2.1 proteins in native tissues by immunoblotting, respectively.

Immunoprecipitation and Immunoblotting in PC-12 Cells. IP has been described in detail (Michaelevski et al., 2003). In brief, cells were suspended in 5 ml of lysis buffer [20 mM Tris, pH 7.5, 5 mM EDTA, 100 mM EGTA, 100 mM NaCl, and 1% Triton X-100 supplemented with protease inhibitor cocktail (Boehringer-Mannheim)], incubated for 1 h at 4°C, and centrifuged for 10 min at 4°C at 14,000 rpm. After overnight incubation of the supernatant with antibodies at 4°C, protein A-Sepharose beads (Zymed, South San Francisco, CA) were added, and the bound proteins were thoroughly washed (in phosphate-buffered saline with only 0.1% Triton X-100), separated by SDS-PAGE, and subjected to Western blot analysis

using the Amersham ECL detection system (GE Healthcare, Little Chalfont, Buckinghamshire, UK).

Immunoprecipitation in Oocytes. Oocytes were subjected to immunoprecipitation as described previously (Levin et al., 1995). In brief, immunoprecipitates from 1% Triton X-100 oocyte homogenates were analyzed by SDS-polyacrylamide gel electrophoresis (PAGE; 8% polyacrylamide). Digitized scans were derived by PhosphorImager (Molecular Dynamics, Sunnyvale, CA), and relative intensities were quantified by ImageQuant software.

Confocal Immunofluorescence Microscopy. This was done as previously described for HEK-293 cells transfected with Kv2.1 cDNA using lipofectamine 2000 (Invitrogen Canada Inc., Burlington, ON, Canada) (MacDonald et al., 2002) and for pancreatic tissue sections (Wheeler et al., 1996; Pasyk et al., 2004). Pancreatic tissue sections (10 μm thick) from male Sprague-Dawley rats (200 g) were plated on glass coverslips, fixed with 2% paraformaldehyde, and rinsed in phosphate-buffered saline for 5 min. These were then blocked with 5% normal goat serum with 0.1% saponin for 0.5 h at room temperature and then washed and incubated with the indicated paired primary antibodies (1:50 dilution) for 1 h, including rabbit antibodies to either Kv2.1-C terminus or Kv2.1/Kv2.2-N terminus, against guinea pig anti-insulin (gift from Ray Pederson, University of British Columbia, Vancouver, BC, Canada), mouse anti-glucagon (Sigma, St. Louis, MO), or mouse anti-somatostatin (GeneTex, San Antonio, TX) antibodies. This is then followed by appropriate paired fluorochrome (fluorescein isothiocyanate or Texas Red)-conjugated secondary antisera (Jackson ImmunoResearch Laboratories Inc., West Grove, PA) for 1 h at 25°C. The coverslips were then mounted on slides in a fading retarder- 0.1% *p*-phenylenediamine in glycerol, and examined using a laser scanning confocal imaging system (LSM 410; Carl Zeiss, Oberkochen, Germany).

Oocytes and Electrophysiological Recording. *X. laevis* oocytes were prepared as described previously (Ivanina et al., 1994). Oocytes were injected with 0.05 to 0.25 or 10 ng/oocyte Kv2.1 and Kv2.2 mRNAs for electrophysiological and biochemical experiments, respectively. Syntaxin 1A mRNA was injected at 0.5 to 7.5 and at 5 ng/oocyte for electrophysiological and biochemical experiments, respectively. SNAP-25 mRNA was injected at 0.5 to 15 and at 15 ng/oocyte for electrophysiological and biochemical experiments, respectively. BoNT/A mRNA was injected for both biochemical and electrophysiological experiments at 5 to 15 ng/oocyte. AS-ODN at 0.05 ng/oocyte was injected 2 days before the electrophysiological assay, which was done 3 days after the mRNA injection. Two-electrode voltage clamp recordings were performed as described previously (Levin et al., 1995). To avoid possible errors introduced by series resistance, only current amplitudes up to 4 μA were recorded. Net current was obtained by subtracting the scaled leak current elicited by a voltage step from −80 to −90 mV. Oocytes with a leak of more than 3 nA/mV were discarded. Experimental protocols are described in the figure legends.

Data Analysis. For inactivation, data from each oocyte were fitted to a Boltzmann equation: $I/I_{max} = 1/1 + [\exp(Vi_{1/2} - V)/a]$, and mean values for half-inactivation voltage ($Vi_{1/2}$) and for the slope factor (a) were derived. For activation, data from each oocyte were fitted to a Boltzmann equation: $G/G_{max} = 1/1 + [\exp(Va_{1/2} - V)/a]$. Parameters describing the activation curves of groups injected with channel together with syntaxin 1A were obtained by fitting the data to a two-component Boltzmann equation: $G/G_{max} = b/(1 + [\exp(Va_{1/2\_1} - V)/a_1]) + (1 - b)/(1 + [\exp(Va_{1/2\_2} - V)/a_2])$, where G/G_{max} is normalized conductance, $Va_{1/2\_1}$ and $Va_{1/2\_2}$ are half-activation voltages, and a_1 and a_2 are slope factors.

Data are presented as means ± S.E.M. The statistical significance

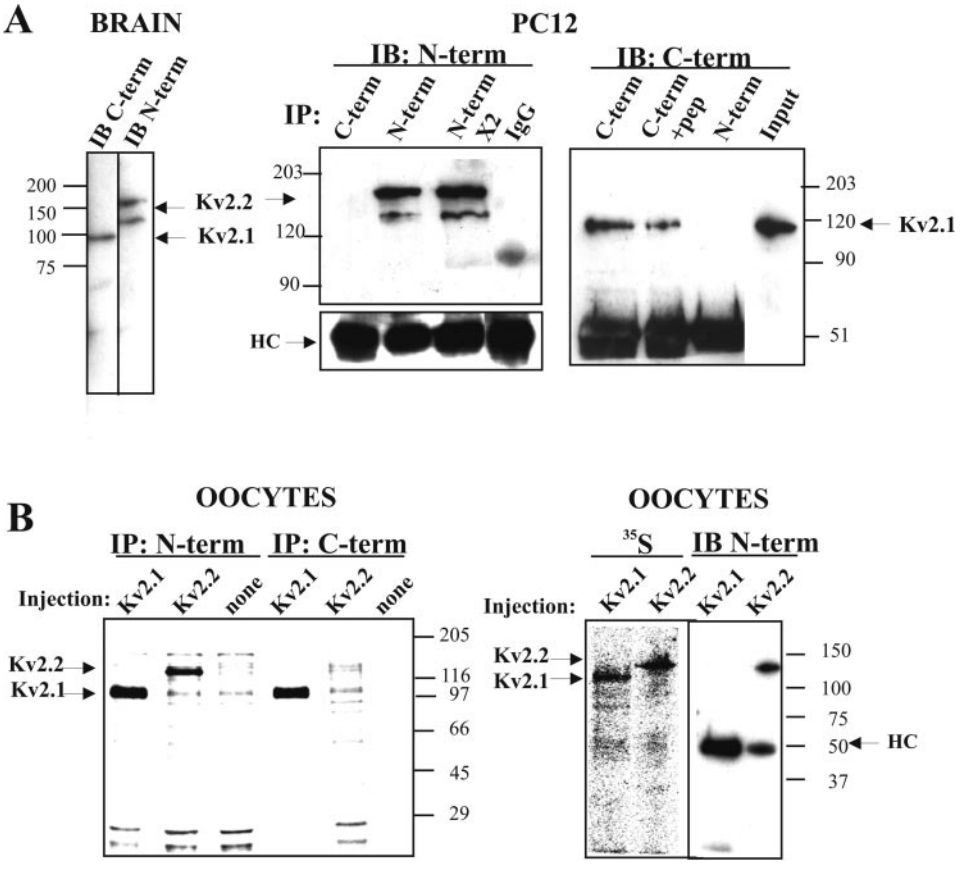

Fig. 1. Characterization of a new antibody that recognizes native Kv2.2 but not Kv2.1. A, the antibody directed against the C terminus of Kv2.1 (C-term) recognizes Kv2.1 but not Kv2.2, whereas the antibody directed against the N termini of Kv2.1 and Kv2.2 (N-term) recognizes Kv2.2 but not Kv2.1, both in brain lysate (left) and PC-12 cells (right two). Left, 10 μg of rat brain tissue solubilized in SDS sample buffer was separated by SDS-PAGE, blotted, and detected by antibodies (IB), as indicated above the blots. Kv2.1 migrated around 110 kDa and Kv2.2 migrated as a doublet around 150 kDa. Right, 1% Triton X-100 PC-12 cell lysates were immunoprecipitated (IP) by the antibodies indicated above the lanes (in the absence and presence of antigen peptide (+pep; 1:1 ratio); IgG, irrelevant Ab; X2, double amount), the precipitated proteins were separated by SDS-PAGE, blotted, and detected (IB) by the N-or C-terminal Abs, as indicated above the blots (HC, heavy chain of the Abs used). This is representative of three similar experiments. For each IP reaction, we used 1.5×10^6 cells. PC-12 lysate (input) (3%) was loaded on one lane. B, in *X. laevis* oocytes, the N-terminal Ab can IP both Kv2.1 and Kv2.2 (left) but can IB only Kv2.2 (right). Left, digitized PhosphorImager scan of SDS-PAGE analysis of [^{35}S]Met/Cys-labeled Kv2.1 and Kv2.2 proteins immunoprecipitated (IP) by the Abs indicated above the lanes from 1% Triton X-100 homogenates of oocytes that were either not injected (none), injected with Kv2.1, or injected with Kv2.2 mRNAs. Right, Kv2.1 or Kv2.2 visualized by [^{35}S]Met/Cys scanning, were also blotted with the N-terminal Ab. Molecular mass markers are shown on the sides.

of differences between two groups was calculated by the use of independent sample *t* test procedures assuming unequal variance (Mann-Whitney's rank-sum test). One-way ANOVA was used to estimate the statistical differences in experiments comparing several groups.

Results

Kv2.1 and Kv2.2 Are Distinctly Located in Different Pancreatic Islet Cells. In view of the specificity of the C-terminal and the N-terminal antibodies (Abs) for the recognition by immunoblotting of native Kv2.1 and Kv2.2, respectively (Fig. 1 and *Materials and Methods*), we used them to examine the distinct cellular location of the Kv isoforms within the rat pancreatic islets (Fig. 2). To verify the specificity of the antibodies for confocal microscopy analysis as well, HEK-293 cells expressing the channels were analyzed before examining pancreatic tissue sections. In addition, we used pancreatic tissue sections that showed the surrounding exocrine tissues to contain neither Kv2.1 nor Kv2.2, thereby serving as additional negative controls for both Kv channels and the different antibodies. Figure 2A shows that the C-terminal Ab stained specifically the plasma membrane of HEK-293 cells expressing Kv2.1 (in a–c) but not Kv2.2 (in d and e), as expected. In rat pancreatic islets, the insulin-containing islet β cells, which are more abundant in the central core of the islet, costained with the C-terminal Ab (in f–h). Next, we examined the N-terminal Ab specificity in confocal microscopy analysis. Figure 2B shows that the N-terminal Ab specifically stained Kv2.2 channels overexpressed in HEK-293 cells, because the staining was completely blocked when the antibody was preabsorbed with the peptide against which the antibody was generated (in a–d). It is noteworthy that this antibody did not stain insulin-containing β cells (in e–g), which we showed above to express Kv2.1, thereby verifying that Kv2.1, but not Kv2.2, is present in β cells (MacDonald et al., 2001). We then examined which Kv isoform was present in the rat glucagon-containing α cells and somatostatin-containing δ cells, both of which are predominantly present in the mantle or periphery of the pancreatic islet. Using the N-terminal Ab, we were surprised to find that Kv2.2 were present not only in the δ cells (in k–m), as would be expected, but also in the α cells (in h–j). Kv2.2 mRNA has been consistently shown to be present in human islet δ cells, but the Kv2.2 protein was apparently not explored in the α cells. Unfortunately, we could not get the N-terminal Ab to consistently stain the human pancreatic tissue well, probably because of degradation occurring during organ retrieval and preparation (data not shown). The α and δ cells are rather sparse within the islets and are not readily distinguishable from the β cells when the islets are dispersed into single cells. Whereas all islet cells contain *t*-SNARE proteins (Wheeler et al., 1996), each islet cell contains additional distinct Kv channels besides the dominant forms. Therefore, it would be extremely difficult to directly examine only the dominant Kv channels in these cells and their interactions with SNAREs. Hence, we have used the oocyte expression model to examine how the Kv2.1 and Kv2.2 channels in these different islet cells may be regulated by the *t*-SNARE proteins.

Effects of Syntaxin 1A on the Voltage Dependence and Kinetics of Inactivation of Kv2.2 versus Kv2.1. We have shown that co–injection of low concentration (10 ng/μl) of syntaxin 1A (low syntaxin) mRNA with Kv2.1 mRNA into oocytes affects the steady-state slow inactivation of the outward K^+ currents. The half-inactivation voltage ($Vi_{1/2}$) is shifted to the left with no effect on the residual current fraction (RCF), measured at the end of a 5-s depolarization to +15 mV (Michaelevski et al., 2003). In this study, we examined the dependence of the effect on syntaxin 1A concentration (Fig. 3, A–D). We were surprised to find that the leftward shift of $Vi_{1/2}$ caused by low syntaxin was replaced by a rightward shift in oocytes of the same batch expressing high concentration (2.5 ng/oocyte) of syntaxin 1A (high syntaxin). In addition, high syntaxin, in contrast to low syntaxin, increased the RCF. Neither low nor high syntaxin had a significant effect on the slope factor of the Kv2.1 inactivation curve.

Next, we examined the effect of syntaxin 1A on the steady-state slow inactivation of the outward K^+ currents of the closely related channel Kv2.2 (Fig. 3, E–H). In contrast to Kv2.1, low syntaxin caused only small (if any) leftward shift, whereas high syntaxin (>2.5 ng/oocyte mRNA) caused a statistically significant leftward shift of $Vi_{1/2}$ that was also accompanied by an increase in RCF. In addition, in the presence of high syntaxin, the slope factor of the inactivation curve became more negative.

The effects of syntaxin 1A on the kinetics of onset of inactivation were compared between Kv2.1 and Kv2.2. Inactivation onset was measured as the rate of current decay during 25-s depolarizing pulses and estimated by the inactivation time constant (τ_i) derived from a single exponential decay fit. High syntaxin increased τ_i (slowed down inactivation) of both Kv2.1 and Kv2.2 by approximately 40 to 50%, determined at +10 to +30 mV, whereas low syntaxin had no effect on τ_i (data not shown).

Effects of Syntaxin 1A on the Voltage Dependence and Kinetics of Activation of Kv2.2 versus Kv2.1. In a previous work (Michaelevski et al., 2003), we have shown that low syntaxin affected the steady-state activation of the Kv2.1 channels. Thus, in oocytes coexpressing Kv2.1 with low syntaxin, the activation curve was fitted with two-component Boltzmann function. One component resembled that for the conductance (*G*)-voltage curve of Kv2.1 expressed alone [with the same half-activation voltage ($Va_{1/2}$) and slope factor]. The other component had $Va_{1/2}$, which is strongly shifted to hyperpolarized potentials with a strong decrease in the slope factor of the activation curve, indicating a steeper dependence on voltage (Fig. 4, A–C). In this study, we examined the effect of a high concentration of syntaxin 1A on the steady-state activation of Kv2.1 (Fig. 4, B and C). We were surprised to find that the hyperpolarizing shift by low syntaxin was eliminated in oocytes of the same batch expressing high syntaxin (Fig. 4, A–C).

Next, we examined the effect of syntaxin 1A on the steady-state activation of Kv2.2 (Fig. 4, E–G). In contrast to Kv2.1, low syntaxin had no significant effect on Kv2.2, whereas high syntaxin affected Kv2.2 activation similarly to the effect of low syntaxin on Kv2.1. The activation curve in the presence of high syntaxin was best fitted by a two-component function. One component strongly shifted to hyperpolarized potentials with a strong decrease in slope factor; activation of the second component resembled the activation of Kv2.2 expressed alone. The two components could represent two distinct pop-

ulations of channels, affected and not affected by syntaxin, as suggested previously for Kv2.1 (Michaelevski et al., 2003).

In contrast to Kv2.1, syntaxin 1A affected the activation rate of Kv2.2, (Fig. 4, compare E with A and H with D). Activation time constants were derived from exponential fits to current traces elicited at the denoted voltages. For oocytes expressing Kv2.2 alone, one activation time constant was derived, whereas for oocytes also expressing high syntaxin, two activation time constants were derived. One time constant, τ_{slow}, was the same as that obtained in the absence of syntaxin 1A. The second time constant, τ_{fast}, was significantly smaller and was not voltage-dependent in all voltages

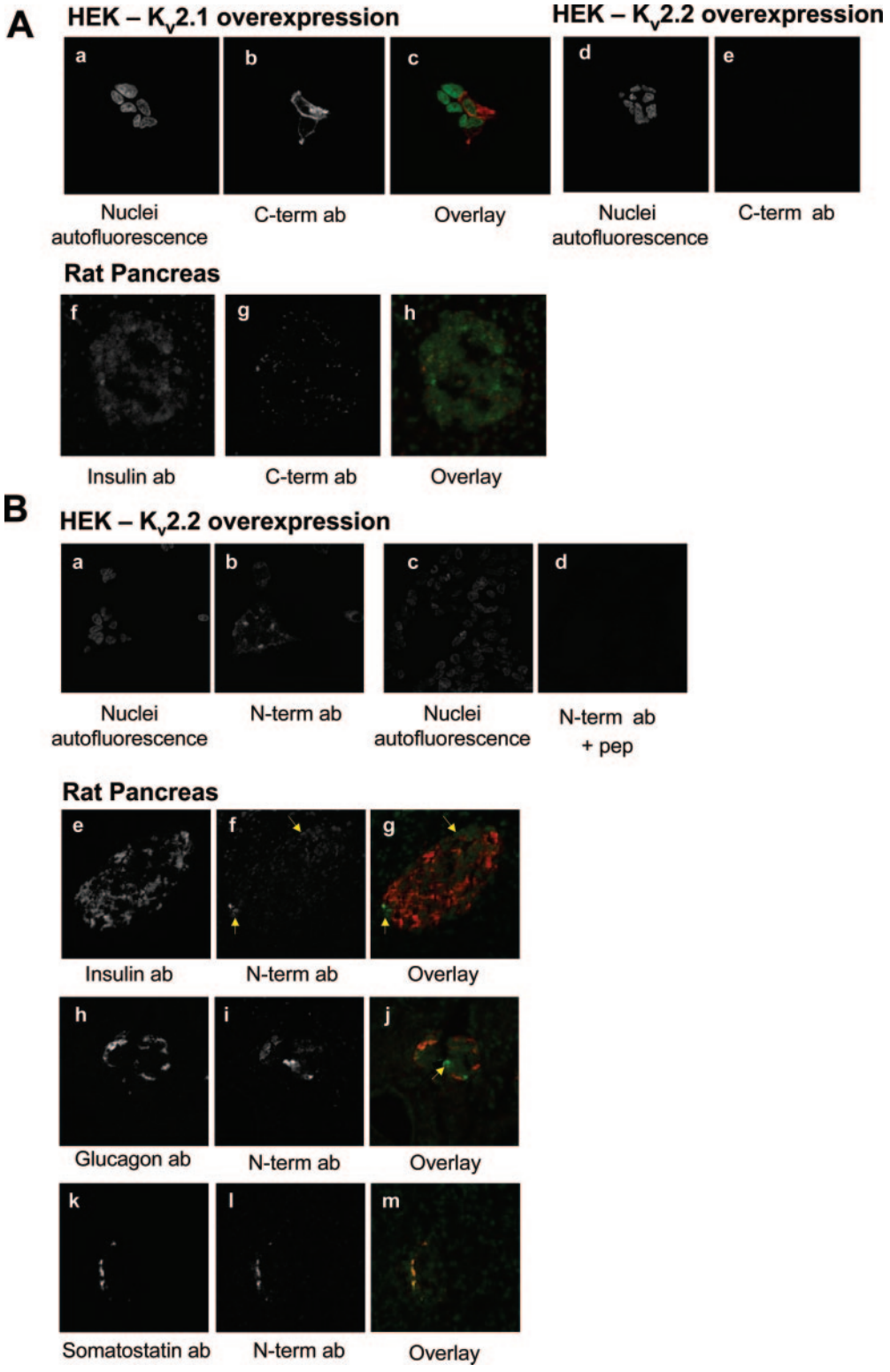

Fig. 2. Kv2.1 and Kv2.2 localization in rat pancreatic islet cells. A, Kv2.1 localization to insulin-containing β cells. C-terminal antibody (b, pseudocolored red in overlay image in c) stains Kv2.1 at the plasma membrane which surrounds the nuclei (a, pseudocolored green in c) of Kv2.1-overexpressing HEK-293 cells. C-terminal antibody does not see Kv2.2 (e) in Kv2.2-overexpressing HEK-293 cells. Note the nuclei staining (a and d) is actually autofluorescence. In rat pancreas sections, insulin antibody (f, pseudocolored green in h) stains the cytosol of majority of islet cells. The C-terminal antibody (g, pseudocolored red in h) stains the same islet beta cells, appearing as adjacent (red) or overlapping (yellow-green) with insulin in the overlay image (h). This is because insulin secretory granules may or may not be docked close to the plasma membrane (where Kv2.1 is located) in the β cells. Note the faint green autofluorescing nuclei of surrounding acinar cells (h) that are not labeled with the C-terminal antibody. B, Kv2.2 localization to glucagon-containing α cells and somatostatin-containing δ cells. N-terminal antibody (b) stains the PM of Kv2.2-overexpressing HEK-293 cells, and this signal is completely blocked when the antibody is first preabsorbed with the blocking peptide (d). The autofluorescent nuclei identify the HEK-293 cells (a and c), which correspond to the translucent cytosolic areas in b. In rat pancreas sections, insulin-containing β cells (e, pseudocolored red in overlay image in g) are not stained by the N-terminal antibody (f, indicated by arrows; pseudocolored green in g), indicating that islet β cells have no or low abundance of Kv2.2. In contrast, islet α cells stained with glucagon antibody (h, pseudocolored red in overlay image in j) and δ cells stained with somatostatin antibody (k, pseudocolored red in overlay image in m) are most abundant in the mantles (not central cores) of islets. These α and δ cells stained with the N-terminal antibody (i and l, pseudocolored green in j and m), which identifies Kv2.2 on the plasma membrane, and which in overlay images (j and m) appeared either adjacent (green in j) or overlapping (yellow in m) with the staining by glucagon or somatostatin antibodies (both in red). The latter is the case because secretory granules may or may not be docked close to the plasma membrane in these cells. The arrow in j points to a cell with Kv2.2 and no adjacent glucagon, which is probably a δ cell. Note the autofluorescing nuclei of the surrounding acinar cells (f, i, and l), which appear faint green in the overlay images (g, j, and m), and these acinar cells were not labeled with the N-terminal antibody.

tested. The two time constants may indicate two populations of channels: affected and not affected by syntaxin. No significant changes in current amplitudes were observed in either Kv2.1 or Kv2.2 channels, in the presence of low or high concentrations of syntaxin.

Effects of SNAP-25, Alone and in Combination with Syntaxin, on the Inactivation of Kv2.2. We have shown previously that coexpression of SNAP-25 with Kv2.1 shifted the $Vi_{1/2}$ to depolarized potentials, enhanced RCF, and increased τ_i (Michaelevski et al., 2003). Furthermore, we

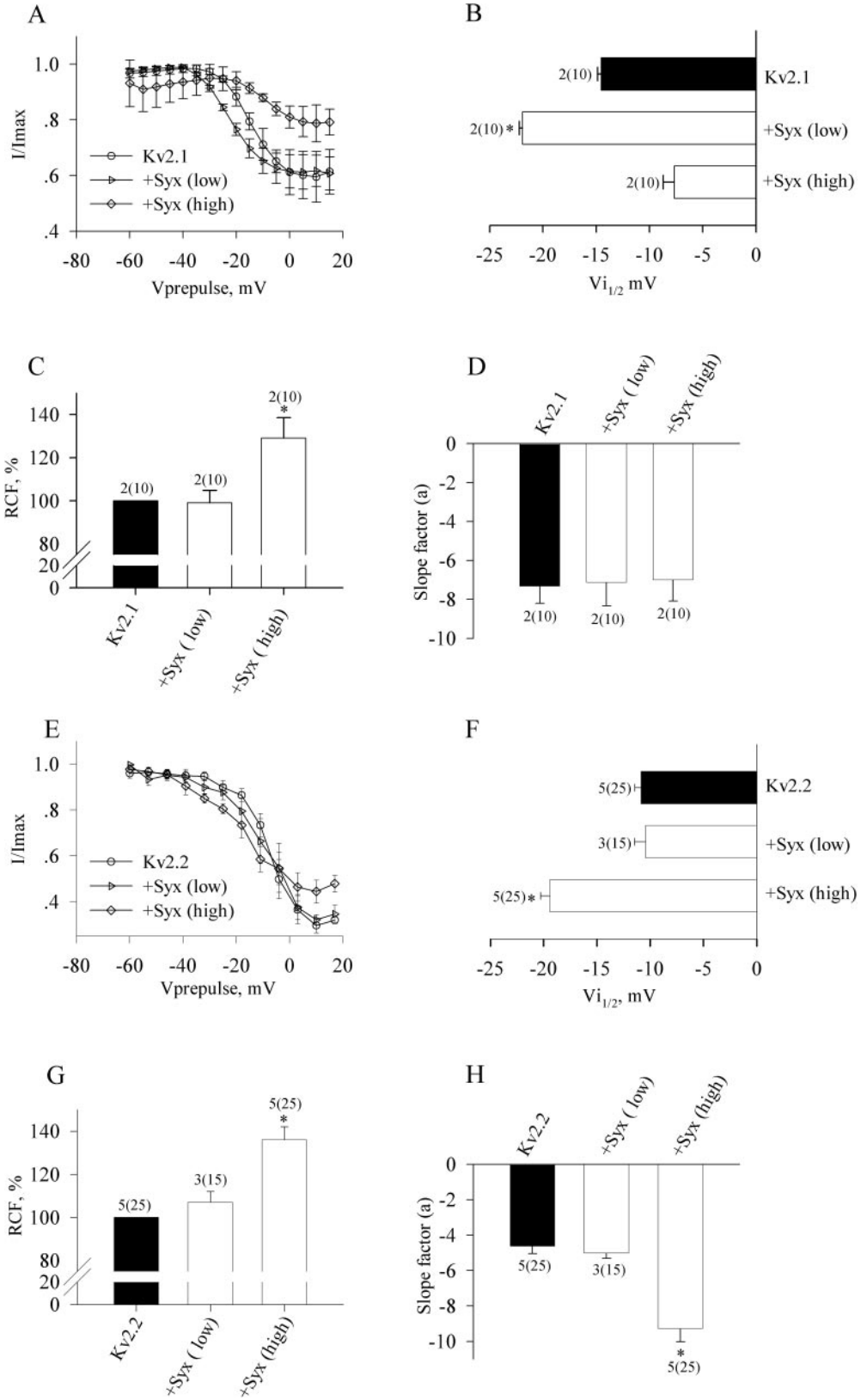

Fig. 3. Effects of syntaxin 1A on the voltage dependence of the steady-state inactivation of Kv2.2 versus Kv2.1. Oocytes injected with Kv2.1 alone (Kv2.1), with low (0.5 ng/oocyte) syntaxin 1A [+Syx (low)] or with high (>2.5 ng/oocyte) syntaxin [+Syx (high)] mRNAs were tested. A, a representative experiment in a single batch of oocytes with five oocytes per group demonstrating the effects of syntaxin on the steady-state inactivation of Kv2.1. Currents were derived by 5-s depolarizing prepulses (Vprepulse) applied from −80 mV in ascending order, followed by a 120-ms test pulse to +50 mV. Mean fractional currents (I/I_{max}) were plotted as function of Vprepulse. Data from each oocyte were fitted to a Boltzmann equation and mean parameters of inactivation drawn from several experiments are shown in B to D. B, mean values of half-inactivation potential ($Vi_{1/2}$). C, mean values of RCF. D, mean values of slope factor. E–H, the same as in A–D, respectively, but with Kv2.2. In all bar diagrams, numbers without and with parentheses denote number of batches and total number of oocytes per group; the same batches were tested for all groups. *, $p < 0.01$.

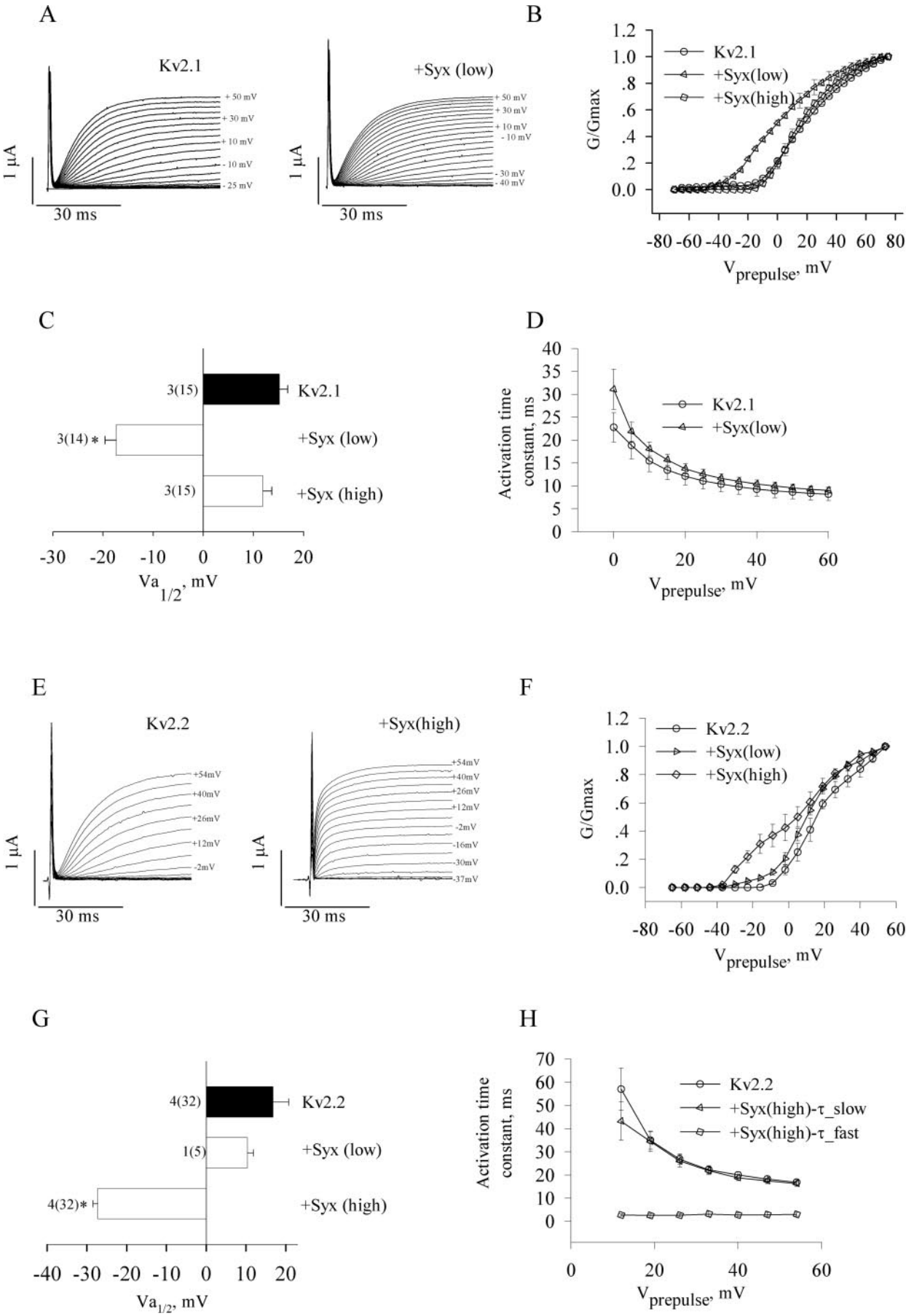

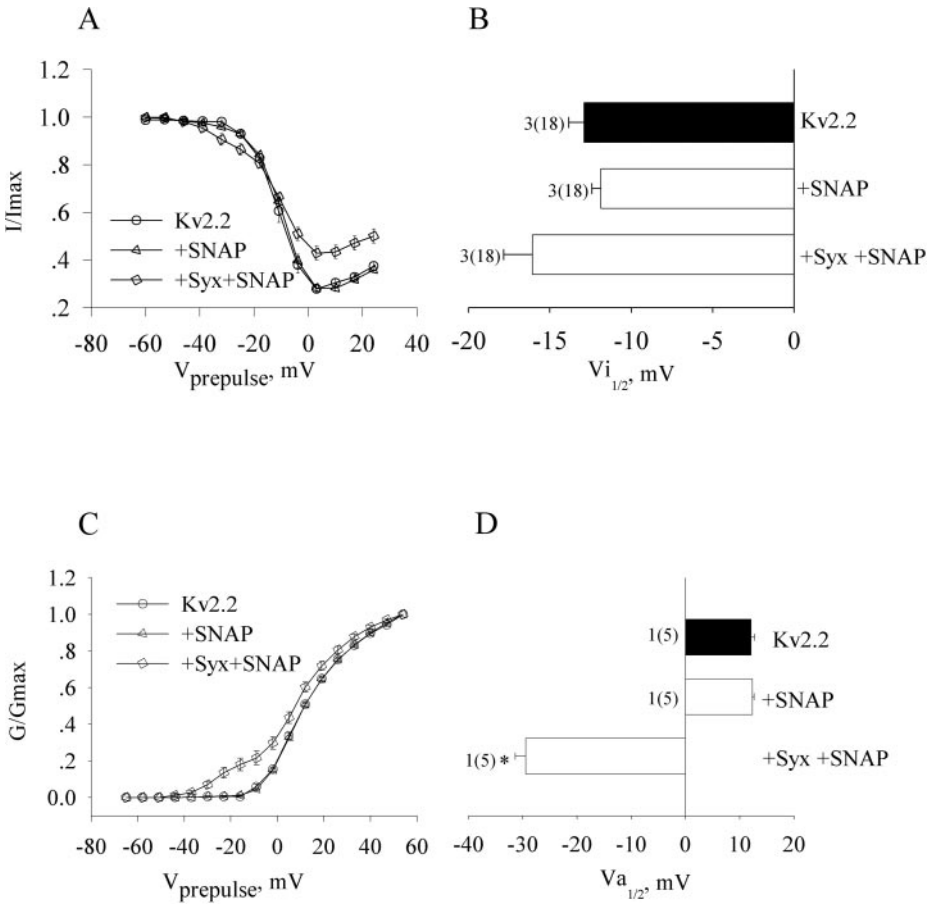

Fig. 5. Effects of syntaxin 1A, SNAP-25 and a combination of syntaxin 1A and SNAP-25 on the inactivation and activation of Kv2.2. Oocytes injected with Kv2.2 alone (Kv2.2), or together with SNAP-25 (+SNAP) or combination of syntaxin 1A and SNAP-25 (+Syx+SNAP) were tested for steady-state inactivation (A and B) or activation (C and D). Experiments and analyses were performed as described in Figs. 1 and 2. Mean $Vi_{1/2}$ and $Va_{1/2}$ values are shown in bar charts. Numbers without and with parentheses denote number of batches and total number of oocytes per group; the same batches were tested for all groups. *, $p <$ 0.01.

showed that combination of SNAP-25 with syntaxin 1A diminished the hyperpolarizing shift of $Vi_{1/2}$ caused by low syntaxin and replaced it by a depolarizing shift, similar to the effect of SNAP-25 alone. Here, we examined the effects of SNAP-25, alone and in combination with high syntaxin (which is effective on Kv2.2), on Kv2.2 inactivation. In contrast to Kv2.1, Kv2.2 steady-state inactivation and τ_i (data not shown) were not affected by SNAP-25 alone. In addition, SNAP-25, in combination with syntaxin, did not shift $Vi_{1/2}$ to depolarized potentials (Fig. 5, A and B). Occasionally, however, the enhancement by syntaxin 1A of RCF was increased in the presence of SNAP-25.

Effects of SNAP-25, Alone and Combined with Syntaxin 1A, on the Activation of Kv2.2. We have shown that SNAP-25 alone had no effect on Kv2.1 activation (Michaelevski et al., 2003); however, combined with syntaxin 1A, it diminished the hyperpolarizing shift caused by low syntaxin. Here, we examined the effects of SNAP-25, alone and in combination with high syntaxin, on Kv2.2 activation (Fig. 5, C and D). SNAP-25 alone had no effect on Kv2.2 activation, as with Kv2.1. However, in contrast to Kv2.1, in the presence of SNAP-25 and syntaxin 1A, the hyperpolarizing shift was apparent.

Physical Interactions of Syntaxin 1A and SNAP-25 with Kv2.2. Physical interactions were examined by coimmunoprecipitation analysis in oocytes, using antibody against Kv2.2. Figure 6 shows that in oocytes coinjected with Kv2.2 and syntaxin, syntaxin 1A coprecipitated with Kv2.2. However, in oocytes injected with Kv2.2 and SNAP-25, the coprecipitation of SNAP-25 was weak (if any).

High Syntaxin, SNAP-25, and Their Combination Act in the Context of the Syntaxin/SNAP-25 Complex in the Case of Kv2.1. The effects of coexpressed low syntaxin, high syntaxin, SNAP-25, and syntaxin+SNAP-25 on activation and inactivation parameters of Kv2.1 are summarized qualitatively in Table 1. The effects of high syntaxin, SNAP-

Fig. 4. Effects of syntaxin on the steady-state and kinetics of activation of Kv2.2 versus Kv2.1. Oocytes injected with either Kv2.1 alone or together with low or high syntaxin (abbreviations as in Fig. 1) were tested. A, representative current traces in single oocytes from a single batch injected with either Kv2.1 alone or with low syntaxin. B, a representative experiment in a single batch of oocytes with five oocytes per group demonstrating the effects of syntaxin 1A on the steady-state activation of Kv2.1 in the three groups of oocytes tested. Normalized conductance (G/G_{max})-voltage relationships were derived from current-voltage relationships obtained from peak currents elicited by 300-ms steps to the denoted potentials (with interval of 1 s between episodes). G values were obtained from the peak currents, assuming a reversal potential of −98 mV for K^+ ions. Mean data were fitted to one component (Kv2.1 alone and with high syntaxin) or two-component (Kv2.1 with low Syntaxin) Boltzmann equation. C, bar chart showing the mean half-activation ($Va_{1/2}$) values derived from several experiments (for low syntaxin the component that is different from the values of the other groups is shown). D, activation time constants derived from one-exponential fits to the rising phase of currents elicited at different potentials. E–H, the same experiments and analyses were performed for oocytes injected with Kv2.2, either alone or together with low or high syntaxin. Mean data were fitted to one component (Kv2.2 alone and with low syntaxin) or two-component (Kv2.2 with high syntaxin) Boltzmann equation (F) (for the high syntaxin group the component that is different from the values of the other groups is shown in G). Two activation time constants were derived from bi-exponential fit for high syntaxin group (H). In all bar diagrams, numbers without and with parentheses denote number of batches and total number of oocytes per group; the same batches were tested for all groups.* $p < 0.01$.

25, and syntaxin 1A/SNAP-25 seem strikingly similar (and distinct from those by low syntaxin). We have shown previously that in both syntaxin+SNAP-25 and SNAP-25 coexpressions, syntaxin 1A/SNAP-25 complexes are being formed (in the latter case, SNAP-25 associates with endogenous syntaxin) and exert their effects on the channel (Michaelevski et al., 2003). Thus, because the effects by high syntaxin were similar to those exerted by the syntaxin/SNAP-25 complexes, we set out to examine whether they are dependent on endogenous SNAP-25 and thus may be attributable to complexes of syntaxin 1A with endogenous SNAP-25.

To this end, we knocked down endogenous SNAP-25 using two approaches and assayed the effects of high syntaxin. First, we expressed the light chain of BoNT/A, which cleaves the last nine residues from the C terminus of SNAP-25 (Turton et al., 2002) and was shown by us to cleave SNAP-25 expressed in oocytes (Michaelevski et al., 2003). The functional efficiency of BoNT/A was verified by the large reduction of the effects of coexpressed SNAP-25: enhancement of the RCF was weakened by ~70%, the depolarizing shift of $Vi_{1/2}$ was abolished (Fig. 7A), and the increase in τ_i was

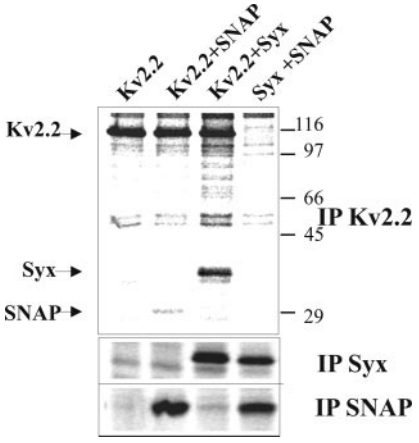

Fig. 6. Physical interactions of syntaxin 1A and SNAP-25 with Kv2.2 in oocytes. Top, digitized PhosphorImager scan of SDS-PAGE analysis of [^{35}S]Met/Cys-labeled Kv2.2, syntaxin 1A and SNAP-25 proteins coimmunoprecipitated by the N-terminal antibody (IP Kv2.2) from 1% Triton X-100 homogenates of oocytes that were injected with Kv2.2 mRNA (15 ng/oocyte) only, coinjected with either syntaxin 1A (5 ng/oocyte) or SNAP-25 (15 ng/oocyte) mRNAs, or injected with syntaxin 1A and SNAP-25 together (without Kv2.2), as indicated above the lanes. Arrows indicate the relevant proteins. Numbers indicate molecular mass markers. Bottom, immunoprecipitation by syntaxin 1A (IP Syx) or by SNAP-25 (IP SNAP-25) antibodies from the same groups of oocytes as in the top. The results shown are from one of three independent experiments.

TABLE 1
Qualitative effects of Syntaxin 1A, SNAP-25, and the combination of syntaxin 1A and SNAP-25 on the activation and inactivation of Kv2.1 vs. Kv2.2

	Kv2.1					Kv2.2				
	Activation		Inactivation			Activation		Inactivation		
	$Va_{1/2}$	τ_a	$Vi_{i1/2}$	RCF	τ_i	$Va_{1/2}$	τ_a	$Vi_{i1/2}$	RCF	τ_i
Low syntaxin	←	X	←	X	X	X	X	X	X	X
High syntaxin	X	X	X/→	↑	↑	←	↑	←	↑	↑
SNAP-25	X	X	→	↑	↑	X	X	X	X	X
Syntaxin + SNAP-25	X	X	→	↑	↑	←	↑	←	↑	↑

τ_a, activation time constant; τ_i, inactivation time constant; ← , leftward shift to more hyperpolarized voltages; X, no effect; X/→ , elimination of the leftward shift and possible rightward shift; ↑ , increase of the specified parameter; → , rightward shift to more depolarized voltages.

inhibited by ~90% (not shown). Next, we examined the effect of high syntaxin in the presence of BoNT/A. As shown in Fig. 7B, coexpression of BoNT/A with high syntaxin abolished the depolarizing shift of $Vi_{1/2}$, reduced by ~60% the enhancement of RCF, and inhibited by ~65% the increase in τ_i (data not shown). When the channel was expressed alone, coexpression of BoNT/A had no significant effect on the RCF or on the $Vi_{1/2}$ (data not shown). These results support the notion that the ability of high syntaxin to affect inactivation requires the presence of endogenous SNAP-25.

In the second approach, endogenous SNAP-25 was knocked down using two AS-ODNs, ASNP-1 and ASNP-2, directed against the most highly conserved domains among SNAP-25 proteins from different species (see *Materials and Methods*). A nonsense ODN (NS) of scrambled nucleotide sequence was used as a control. The disadvantage of this approach over the BoNT/A approach is that whereas the toxin targets the whole protein pool, the antisense targets the mRNA and hence only the newly synthesized proteins. First, the efficiencies of the AS-ODNs ASNP-1 and ASNP-2 were verified by demonstrating their ability to knock down expressed SNAP-25 protein, which was not degraded by the NS ODN (Fig. 7D). Then, we tested the effects of the AS-ODNs on the effects of high syntaxin (Fig. 7C). Injection of 50 pg of either of the AS-ODNs into oocytes coexpressing high syntaxin diminished the increased RCF, whereas 50 pg of NS had statistically insignificant effect. Both AS-ODNs shifted $Vi_{1/2}$ slightly to the left (~3 mV) in oocytes coexpressing syntaxin 1A; data not shown). In oocytes expressing Kv2.1 alone, ASNP-2 had no effect on the RCF and had inconsistent effects on $Vi_{1/2}$ (data not shown).

The results of these SNAP-25-knockout experiments were in accord with our notion (see above) that the effects of high syntaxin on Kv2.1 result from recruitment of endogenous SNAP-25 to the channel. Thus, the effects of high syntaxin, SNAP-25, or syntaxin+SNAP-25 reflect effects by the *t*-SNARE complex. This confirms our suggestion (Michaelevski et al., 2003) that the Kv2.1 channel is a target for either syntaxin 1A alone (low syntaxin) or the *t*-SNARE complex, because each exerts distinct effects on the activation and inactivation of the channel (Table 1).

As expected from the lack of any significant effect by SNAP-25 alone on Kv2.2 (Fig. 5 and Table 1, right), BoNT/A did not reduce the effects of high syntaxin on Kv2.2 (data not shown), in contrast to Kv2.1. Thus, it seems that Kv2.2 interacts with syntaxin 1A regardless of its association with SNAP-25. The ensuing effects are quite similar to those exerted on Kv2.1 by both syntaxin 1A alone and the syntaxin 1A/SNAP-25 complex (Table 1; in Kv2.2, and not in Kv2.1; in addition, the activation rate is enhanced).

Discussion

The above analyses of the effects of the *t*-SNAREs syntaxin 1A and SNAP-25 on Kv2.2 revealed significant differences from those on Kv2.1 (see Table 1). Whereas Kv2.1 interacts with both syntaxin 1A alone and the complex syntaxin 1A/SNAP-25, each interaction is manifested by distinct effects on the channel's gating, Kv2.2 seems to interact with syntaxin 1A only, either monomeric or in the context of the complex syntaxin/SNAP-25. The effects of syntaxin 1A on Kv2.2 also comprise some of the effects of the complex on

Kv2.1. In addition, syntaxin 1A enhances the activation rate and decreases the voltage sensitivity of inactivation of Kv2.2, but not of Kv2.1.

The sites of interaction of syntaxin 1A and the syntaxin/SNAP-25 complex with Kv2.1 were previously mapped to the C terminus of the channel (Michaelevski et al., 2003). The site of syntaxin 1A was further mapped down to the proximal quarter of the C terminus (C1a domain) (Tsuk et al., 2005). Kv2.1 and Kv2.2 display high amino acid homology (84.2% amino acid identity) in their N-terminal cytoplasmic domains, core hydrophobic transmembrane regions, and their C1a domains. Thus, it is not surprising that Kv2.2, which harbors a C1a domain that displays 71.9% homology with that of Kv2.1, interacts functionally and physically with syntaxin 1A. However, the differences in the effects of syntaxin 1A between the two channels and the lack of interaction of the syntaxin/SNAP-25 complex with Kv2.2 versus Kv2.1 may be attributed to the involvement of amino acid sequences downstream to threonine 535 or 550 in Kv2.1 or Kv2.2, respectively, which display only 21% identity.

What would be the consequences of these differences on the physiology of cells expressing Kv2.1 versus Kv2.2? As discussed previously (Michaelevski et al., 2003), in cells expressing Kv2.1 (e.g., islet β cells) there is a high probability that at resting membrane potential, the channel is associated with syntaxin 1A because of the the high affinity of syntaxin 1A to Kv2.1 and its high abundance. The association with syntaxin 1A shifts the window of voltages at which the channel conducts ("conductivity window"; derived from superposition of the activation and inactivation curves, see (Michaelevski et al., 2003) to hyperpolarized potentials close to the resting potential, stabilizing membrane potential and reducing cell excitability. However, assembly of syntaxin 1A with SNAP-25 (possibly within the context of the whole SNARE complex formation at spots of docked vesicles ready for release) and the interaction of the *t*-SNARE complex with Kv2.1 shifts the conductivity window to depolarized potentials, enhancing excitability and repolarization of action potentials, thereby facilitating bursting electrical activity. It is noteworthy that in cells expressing the Kv2.2 channel (e.g., islet α- and δ cells), which is not sensitive to the assembly of syntaxin 1A with SNAP-25, the assembled *t*-SNARE complexes, at sites of docked vesicles, are not expected to relieve the membrane potential stabilizing effect conferred by syn-

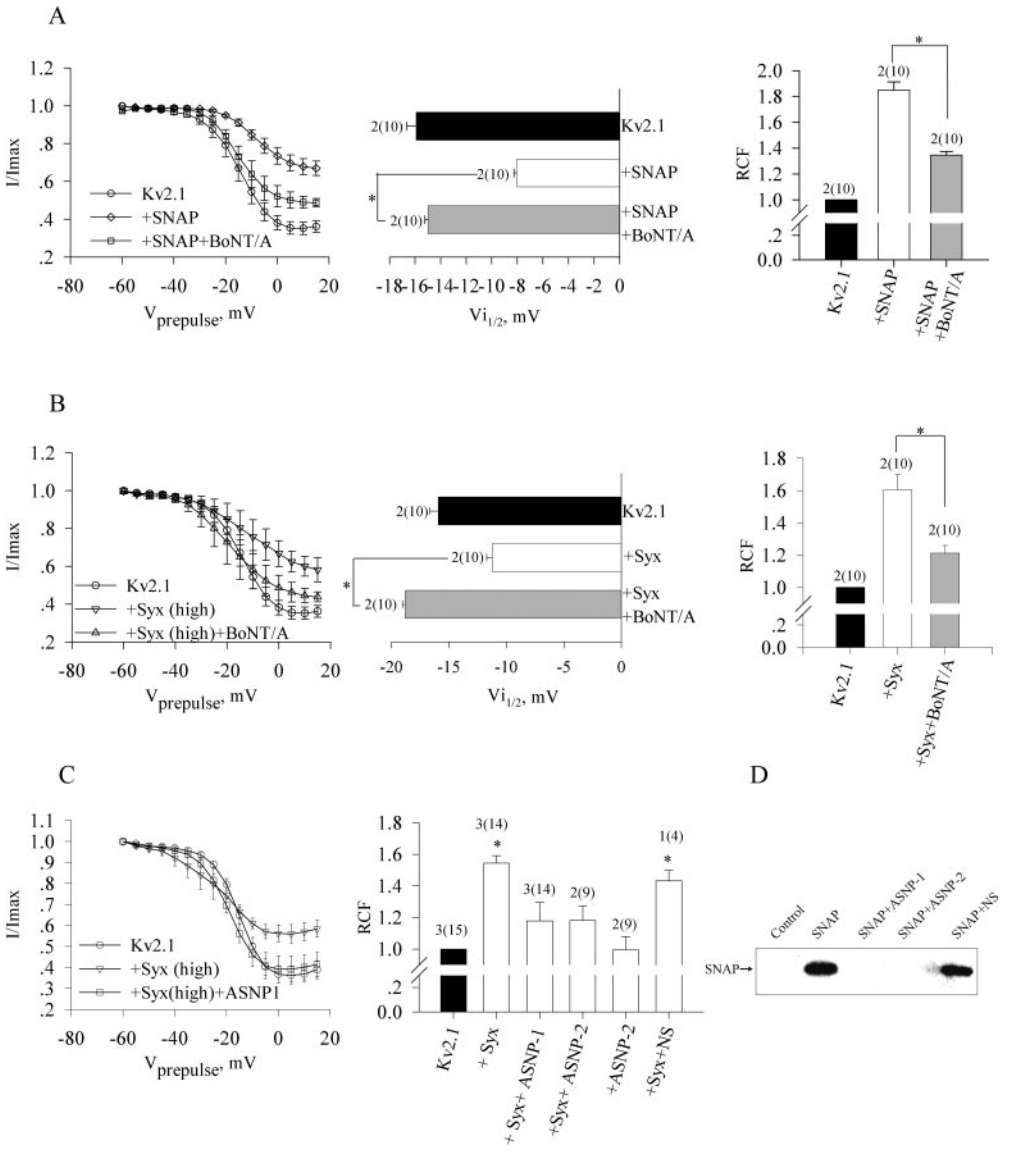

Fig. 7. Knock down of endogenous SNAP-25 reduces the effect of high syntaxin on Kv2.1. A, effect of BoNT/A on the modulation of the steady-state inactivation of Kv2.1 by SNAP-25. Oocytes injected with Kv2.1 alone (Kv2.1) or together with SNAP-25 (+SNAP-25) or with a combination of SNAP-25 and BoTN/A (+SNAP-25+BotA) were tested for their inactivation characteristics. Left, a representative experiment in a single batch of oocytes with five oocytes per group. The right two bar charts show the mean effects on $Vi_{1/2}$ and normalized RCF. B, effect of BoNT/A on the modulation of the inactivation of Kv2.1 by high syntaxin. Oocytes injected with Kv2.1 alone (Kv2.1) or together with syntaxin 1A [+Syx (high)] or with a combination of syntaxin 1A and BoNT/A (+Syx (high)+BoNT/A) were tested for their inactivation characteristics; graph and bar charts are as in A. C, effect of an antisense SNAP-25 ODN (ASNP-1) on the modulation of the inactivation by syntaxin 1A (left) in a single batch of oocytes and the effects of two antisense ODNs (ASNP-1, ASNP-2) on the mean normalized RCF values (right) of Kv2.1 currents. Oocytes were injected 2 days before the assay with Kv2.1 mRNA, alone or together with syntaxin 1A mRNA or together with syntaxin 1A mRNA and the antisense ODN. In all bar diagrams, numbers without and with parentheses denote number of batches and total number of oocytes per group; the same batches were tested for all groups. $* p < 0.01$. D, Western blot analysis of the effect of antisense ODNs on exogenous SNAP-25. Homogenates of whole oocytes injected with SNAP-25, with or without 30 ng of either ASNP-1, ASNP-2 (30 pg) or a nonsense ODN were immunoblotted for SNAP-25.

taxin 1A. However, we expect that such cells will be less susceptible to these effects, either because of their relatively very high input resistance [e.g., islet δ cell; (Gopel et al., 2000a)] or because the voltage range of their resting potential and the threshold of action potential that is more negative than that of the conductivity window of Kv2.2 associated with the *t*-SNAREs [e.g., islet α cells; (Gopel et al., 2000b)]. The hyperpolarizing shift of the conductivity window upon Kv2.2-t-SNAREs complex formation may affect the bursting pattern of action potentials by reducing the amplitude of individual action potentials and increasing intraburst intervals.

The distinct Kv2.1/Kv2.2 distribution among neighboring excitable cells in the brain, in various peripheral tissues and in neuroendocrine cells (Sharma et al., 1993; Barry et al., 1995), specifically among the different types of pancreatic islet cells (see Introduction and this study), suggests that these channels might affect interneuronal or interendocrine cell communication (paracrine control), which could be disrupted by impaired expression levels of SNARE proteins occurring in Diabetes (Ostenson et al., 2006) and a number of neurodegenerative diseases (for example, see Honer et al., 2002).

References

Barry DM, Trimmer JS, Merlie JP, and Nerbonne JM (1995) Differential expression of voltage-gated K^+ channel subunits in adult rat heart. Relation to functional K^+ channels? *Circ Res* **77:**361–369.

Catterall WA (2000) Structure and regulation of voltage-gated Ca^{2+} channels. *Annu Rev Cell Dev Biol* **16:**521–555.

Cejvan K, Coy DH, and Efendic S (2003) Intra-islet somatostatin regulates glucagon release via type 2 somatostatin receptors in rats. *Diabetes* **52:**1176–1181.

Chan CB, MacPhail RM, Sheu L, Wheeler MB, and Gaisano HY (1999) Beta-cell hypertrophy in fa/fa rats is associated with basal glucose hypersensitivity and reduced SNARE protein expression. *Diabetes* **48:**997–1005.

Fili O, Michaelevski I, Bledi Y, Chikvashvili D, Singer-Lahat D, Boshwitz H, Linial M, and Lotan I (2001) Direct interaction of a brain voltage-gated K^+ channel with syntaxin 1A: functional impact on channel gating. *J Neurosci* **21:**1964–1974.

Gaisano HY, Ostenson CG, Sheu L, Wheeler MB, and Efendic S (2002) Abnormal expression of pancreatic islet exocytotic soluble *N*-ethylmaleimide-sensitive factor attachment protein receptors in Goto-Kakizaki rats is partially restored by phlorizin treatment and accentuated by high glucose treatment. *Endocrinology* **143:**4218–4226.

Gopel SO, Kanno T, Barg S, and Rorsman P (2000a) Patch-clamp characterisation of somatostatin-secreting δ-cells in intact mouse pancreatic islets. *J Physiol* **528:**497–507.

Gopel SO, Kanno T, Barg S, Weng XG, Gromada J, and Rorsman P (2000b) Regulation of glucagon release in mouse α-cells by K_{ATP} channels and inactivation of TTX-sensitive Na^+ channels. *J Physiol* **528:**509–520.

Honer WG, Falkai P, Bayer TA, Xie J, Hu L, Li HY, Arango V, Mann JJ, Dwork AJ, and Trimble WS (2002) Abnormalities of SNARE mechanism proteins in anterior frontal cortex in severe mental illness. *Cereb Cortex* **12:**349–356.

Huang X, Kang YH, Pasyk EA, Sheu L, Wheeler MB, Trimble WS, Salapatek A, and Gaisano HY (2001) Ca^{2+} influx and cAMP elevation overcame botulinum toxin A but not tetanus toxin inhibition of insulin exocytosis. *Am J Physiol* **281:**C740–C750.

Ishihara H, Maechler P, Gjinovci A, Herrera PL, and Wollheim CB (2003) Islet beta-cell secretion determines glucagon release from neighbouring alpha-cells. *Nat Cell Biol* **5:**330–335.

Ivanina T, Perets T, Thornhill WB, Levin G, Dascal N, and Lotan I (1994) Phosphorylation by protein kinase A of RCK1 K^+ channels expressed in *Xenopus* oocytes. *Biochemistry* **33:**8786–8792.

Ji J, Tsuk S, Salapatek AM, Huang X, Chikvashvili D, Pasyk EA, Kang Y, Sheu L, Tsushima R, Diamant N, et al. (2002) The 25-kDa synaptosome-associated protein (SNAP-25) binds and inhibits delayed rectifier potassium channels in secretory cells. *J Biol Chem* **277:**20195–20204.

Kang Y, Leung YM, Manning-Fox JE, Xia F, Xie H, Sheu L, Tsushima RG, Light PE, and Gaisano HY (2004) Syntaxin-1A inhibits cardiac KATP channels by its actions on nucleotide binding folds 1 and 2 of sulfonylurea receptor 2A. *J Biol Chem* **279:**47125–47131.

Kanno T, Gopel SO, Rorsman P, and Wakui M (2002) Cellular function in multicellular system for hormone-secretion: electrophysiological aspect of studies on alpha-, beta- and delta-cells of the pancreatic islet. *Neurosci Res* **42:**79–90.

Leung YM, Kang Y, Gao X, Xia F, Xie H, Sheu L, Tsuk S, Lotan I, Tsushima RG, and Gaisano HY (2003) Syntaxin 1A binds to the cytoplasmic C terminus of Kv2.1 to regulate channel gating and trafficking. *J Biol Chem* **278:**17532–17538.

Levin G, Chikvashvili D, Singer-Lahat D, Peretz T, Thornhill WB, and Lotan I (1996) Phosphorylation of a K^+ channel α subunit modulates the inactivation conferred by a β subunit. Involvement of cytoskeleton. *J Biol Chem* **271:**29321–29328.

Levin G, Keren T, Peretz T, Chikvashvili D, Thornhill WB, and Lotan I (1995) Regulation of RCK1 currents with a cAMP analog via enhanced protein synthesis and direct channel phosphorylation. *J Biol Chem* **270:**14611–14618.

MacDonald PE, Ha XF, Wang J, Smukler SR, Sun AM, Gaisano HY, Salapatek AM, Backx PH, and Wheeler MB (2001) Members of the Kv1 and Kv2 voltage-dependent K^+ channel families regulate insulin secretion. *Mol Endocrinol* **15:**1423–1435.

MacDonald PE, Wang G, Tsuk S, Dodo C, Kang Y, Tang L, Wheeler MB, Cattral MS, Lakey JR, Salapatek AM, et al. (2002) Synaptosome-associated protein of 25 kilodaltons modulates Kv2.1 voltage-dependent K^+ channels in neuroendocrine islet beta-cells through an interaction with the channel N terminus. *Mol Endocrinol* **16:**2452–2461.

Michaelevski I, Chikvashvili D, Tsuk S, Fili O, Lohse MJ, Singer-Lahat D, and Lotan I (2002) Modulation of a brain voltage-gated K^+ channel by syntaxin 1A requires the physical interaction of Gβγ with the channel. *J Biol Chem* **277:**34909–34917.

Michaelevski I, Chikvashvili D, Tsuk S, Singer-Lahat D, Kang Y, Linial M, Gaisano HY, Fili O, and Lotan I (2003) Direct interaction of t-SNAREs with the Kv2.1 channel: Modal regulation of channel activation and inactivation gating. *J Biol Chem* **273:**34320–34330.

Ostenson CG, Gaisano H, Sheu L, Tibell A, and Bartfai T (2006) Impaired gene and protein expression of exocytotic soluble N-ethylmaleimide attachment protein receptor complex proteins in pancreatic islets of type 2 diabetic patients. *Diabetes* **55:**435–440.

Pasyk EA, Kang Y, Huang X, Cui N, Sheu L, and Gaisano HY (2004) Syntaxin-1A binds the nucleotide-binding folds of sulphonylurea receptor 1 to regulate the KATP channel. *J Biol Chem* **279:**4234–4240.

Sharma N, D'Arcangelo G, Kleinlaus A, Halegoua S, and Trimmer JS (1993) Nerve growth factor regulates the abundance and distribution of K^+ channels in PC12 cells. *J Cell Biol* **123:**1835–1843.

Spafford JD, Munno DW, Van Nierop P, Feng ZP, Jarvis SE, Gallin WJ, Smit AB, Zamponi GW, and Syed NI (2003) Calcium channel structural determinants of synaptic transmission between identified invertebrate neurons. *J Biol Chem* **278:**4258–4267.

Tsuk S, Michaelevski I, Bentley GN, Joho RH, Chikvashvili D, and Lotan I (2005) Kv2.1 channel activation and inactivation is influenced by physical interactions of both syntaxin 1A and the syntaxin 1A/soluble *N*-ethylmaleimide-sensitive factor-25 (t-SNARE) complex with the C terminus of the channel. *Mol Pharmacol* **67:**480–488.

Turton K, Chaddock JA, and Acharya KR (2002) Botulinum and tetanus neurotoxins: structure, function and therapeutic utility. *Trends Biochem Sci* **27:**552–558.

Wendt A, Birnir B, Buschard K, Gromada J, Salehi A, Sewing S, Rorsman P, and Braun M (2004) Glucose inhibition of glucagon secretion from rat alpha-cells is mediated by GABA released from neighboring beta-cells. *Diabetes* **53:**1038–1045.

Wheeler MB, Sheu L, Ghai M, Bouquillon A, Grondin G, Weller U, Beaudoin AR, Bennett MK, Trimble WS, and Gaisano HY (1996) Characterization of SNARE protein expression in beta cell lines and pancreatic islets. *Endocrinology* **137:**1340–1348.

Yan L, Figueroa DJ, Austin CP, Liu Y, Bugianesi RM, Slaughter RS, Kaczorowski GJ, and Kohler MG (2004) Expression of voltage-gated potassium channels in human and rhesus pancreatic islets. *Diabetes* **53:**597–607.

Address correspondence to: Prof. Ilana Lotan, Department of Physiology and Pharmacology, Sackler Faculty of Medicine, Tel-Aviv University, 69978 Ramat-Aviv. E-mail: ilotan@post.tau.ac.il